MODELLING THE GENERATION AND PROPAGATION OF LANDSLIDE-GENERATED WAVES

J.A. Vasquez[1,2]

1. Northwest Hydraulic Consultants Ltd. (NHC), North Vancouver, British Columbia, Canada
2. jvasquez@nhcweb.com

ABSTRACT

Sub-aerial landslides in water bodies such as bays, fjords, lakes and reservoirs can generate water waves tens or even hundreds of meters high, with potentially devastating effects on infrastructure and human safety. British Columbia has experienced several historic landslide-generated wave events, such as the 20-m high Haney slide wave in the Fraser River (1880); the 25-m high Attachie slide wave in the Peace River (1973) and the recent 35-m high Chehalis Lake wave event (2007). Using the Telemac-2D hydrodynamic model, it is demonstrated that wave propagation results are very sensitive to the mesh resolution and numerical scheme applied to solve the flow equations, typically resulting in excessive wave dissipation (i.e. amplitude under-prediction). It is also shown that correct modelling of these waves requires reproducing the solid slide impacting the water body at high velocity, which is possible using the computational fluid dynamics (CFD) model Flow-3D. It was found in Flow-3D that for accurate of modelling wave propagation over distances larger than 10 times the water depth away from the wave generation region, the use of a second order numerical scheme to solve the momentum advection equations became necessary.

Keywords: landslide-generated waves; CFD; numerical modeling; Flow-3D; Telemac-2D.

1. INTRODUCTION

1.1 Landslide-generated waves and their impacts

Landslides impacting water bodies can generate large impulse water waves, also known as tsunami waves. The landslides can occur completely underwater (sub-aqueous) or above water (sub-aerial), the latter being usually the most relevant because slides falling at high velocity can generate extremely high waves (mega-tsunamis). Figure 1 shows the three phases of sub-aerial landslide-generated waves (Heller et al. 2009): 1) wave generation caused by the impact of slide with the water body; 2) wave propagation radially away from the point of impact accompanied by attenuation of its amplitude; and 3) wave run-up against the shoreline and dam in case of reservoirs (with potential dam overtopping or dam breach).
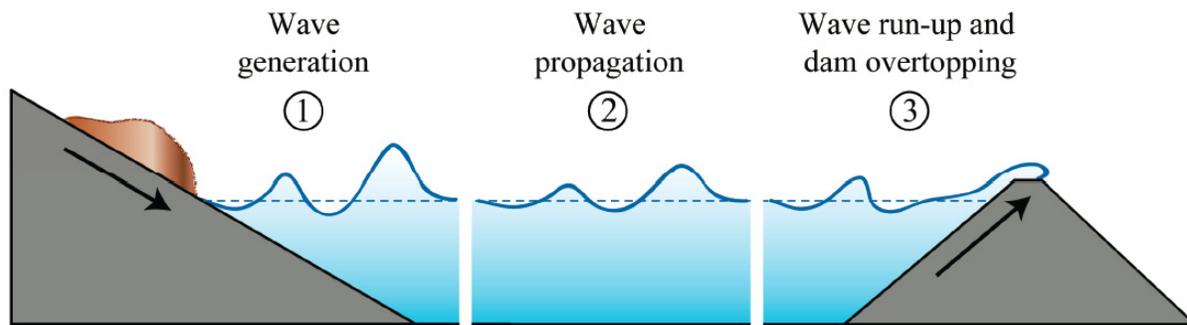
Figure 1. The three phases of landslide-generated waves (Heller et al. 2009).

Table 1 provides some examples of landslide-generated wave events recorded around the world. The largest mega-tsunami wave ever recorded reached 524 m high in Lituya Bay, Alaska (Miller 1960; Fritz et al. 2009). Another well-known case is the 240 m high tsunami wave that overtopped the Vajont Dam in Italy, killing more than 2000 people (Flacker and Eyzaguirre 1979; Wikipedia 2016). The Chungar landslide in Peru caused a 30 m high wave that flooded and destroyed a mining camp, killing an estimated 400 to 600 people (Flacker and Eyzaguirre 1979; Slingerland and Voight 1982). In addition to bays, fiords, lakes, rivers and reservoirs (Table 1); tailings dams and abandoned mining pits flooded with water are also quite susceptible to experience large landslide-generated wave events (Vasquez and de Lima 2006; NHC 2012, 2013, 2016).

Table 1. Examples of historic landslide-generated wave events (Flacker and Eyzaguirre 1979; NHC 1983b; SFU 2011; Wikipedia 2016; Vasquez and de Lima 2016).

Year	Name and location	Slide volume ($\times 10^6$ m^3)	Wave height (m)	Casualties
2008	Three Gorges, China	0.4	32	
2007	Chehalis Lake, BC	3	38	-
2002	Safuna Lake, Peru	20	100	-
1980	Spirit Lake, WA	>2000	260	
1973	Attachie, Peace River, BC	15	25	-
1971	Chungar, Peru	0.1	30	400-600
1963	Vajont Dam, Italy	240	260	2000
1958	Lituya Bay, Alaska	30	524	2
1936	Loen Lake, Norway	1	70	73
1934	Tafjord, Norway	1.5	62	44
1905	Loen Lake, Norway	0.4	40	61
1880	Haney, Fraser River, BC	1	20	1
1792	Shimabara, Japan	535	100	15000+

The province of British Columbia (BC) in Canada has also experienced several landslide-generated wave events. One of the oldest events recorded was the 1880 Haney Slide on the north bank of the Fraser River, 40 km east of Vancouver, when about 1 million m^3 of glacial-marine clay collapsed and moved almost one kilometre across the Fraser River, partially blocking its flow. The wave height was estimated to reach about 20 m high, killing one farmer on the opposite south bank. Fifteen kilometres upstream the wave had attenuated to about 3 m high (SFU 2011; Clague and Turner 2006). The Peace River and tributaries near Fort St. John, where the 60 m high Site C dam is currently under construction, have experience several historic landslides (Van Esch 2012), such as the Attachie slide in 1973 that generated a 25 m high wave in the Peace River (NHC 1983b). More recently in 2007, a large slide entering Chehalis Lake generated a wave that ran up to 38 m in the opposite shore, destroying three empty summer campgrounds. In the Columbia River, the construction of the Revelstoke and Mica hydroelectric dams has increased water levels along the toes of nearly 1000 km of steep mountain slopes, where dozens of large potential rock slides have been identified (Watson et al. 2007), including Downie Slide and Checkerboard, where physical model studies (NHC 1976, 2005) showed that maximum waves heights could potentially exceed 10 m.

Studying and predicting the relevant characteristics of landslide-generated waves for engineering applications is a complex multidisciplinary problem. Geotechnical engineers assess the potential features of the slide, such as location, dimensions, sliding angle and speed, and provide that information to hydrotechnical engineers, who are tasked with predicting the wave hydrodynamics caused by the slide impacting on the water body (Figure 1). Predicted wave information can then be used to determine potential flood extents (impacts lines) around the shores of the water body; assess the risk of dam overtopping; compute outflow hydrographs of water spilling out of the water body and route the floodwave downstream; compute wave forces on structures such as bridge piers; amongst others. Such engineering studies typical involve analyzing several scenarios in which the landslide features or initial water elevations are varied. Mitigation measures can involve geotechnical measures (e.g. slope stabilization, continuous monitoring); protection against wave impact; relocation of people and infrastructure; raising dams or dykes; lowering of water levels; early warning systems; amongst others.

1.2 Predicting wave hydrodynamics

There are three available methods for assessing wave hydrodynamics: analytical equations (Slingerland and Voight 1982; Hughes and Berry 1991; Heller et al. 2009); physical models (NHC 1976, 1983a, 1983b, 2005; Ataie-Ashtani and Nik-Khah 2008; Spheric 2015); and numerical models (Raney and Butler 1975; Basu et al. 2009a,b; Biscarini 2010; Heller et al. 2016; Vasquez and de Lima 2016). Analytical methods are well suited for slide and water bodies of simple geometry, but are less reliable for complex cases, which is why physical modelling has been traditionally applied for important engineering projects; for example, Site C (NHC 1983b) and Revelstoke (NHC 1976, 2005) hydroelectric projects in BC. Numerical models, especially computational fluid dynamics (CFD) models, are now an attractive cost-effective alternative to physical model; but our present knowledge of their real capabilities and limitations is not as mature. The objective of this paper is to provide further insight into the advantages and limitations of numerical modelling for assessing the hydrodynamics of landslide-generated waves. A topic of particular interest is the possibility of numerical dissipation for modelling wave propagation over long distances, which if present in a numerical model would cause the model to underpredict wave amplitude.

Vasquez and de Lima (2016) already proved that the CFD code Flow-3D can accurately reproduce wave generation, propagation and runup in a small basin, intended to represent a flooded mine pit. Although wave patterns were highly three-dimensional and complex, Flow-3D predicted wave runup heights within ±10% of observations made in a physical model, which is quite good for practical applications. However, the length of the basin was only 4 times the water depth and numerical dissipation was likely not issue. Therefore, the need for further verification using the additional experimental data in a long flume (Spheric 2015, Heller et al. 2016), with length in excess of 35 times the water depth where numerical dissipation could be an issue.

The paper is organized as follows. Section 2 provides a brief summary introduction to the numerical modelling of landslide-generated waves. Section 3 describes validation of the Flow-3D CFD model using Heller et al. (2016) experimental data in a long flume. The possibility of modelling wave generation by imposing a known inflow wave boundary condition is explored in Section 4, where the influence of numerical scheme and mesh resolution on wave generation is also illustrated. Summary and conclusions are presented in Section 5. Finally, references are listed at the end in Section 6.

2. NUMERICAL MODELLING

2.1 Wave generation modelling

Conventional depth-averaged hydrodynamic models such as River2D, Telemac-2D and similar could in principle be able to simulate the propagation and runup phases of landslide-generated waves (Figure 1). However, since they lack a mechanism to simulate the transfer of energy and momentum from the solid slide to water, hydrodynamic models cannot simulate the wave generation phase. A very early attempt to deal with this problem was investigated by Raney and Butler (1975), who developed a 2D vertical plane model to simulate the generation and propagation of landslide-generated waves. The moving slide was modelled as a transient bottom deformation which transferred pressure and viscous forces to the liquid by the use of empirical drag equations. The calibrated model reproduced well observations made in a physical model. Although Raney and Butler (1975) semi-empirical approach seemed promising, I was not applied further; perhaps in part because wave generation can now be explicitly solved by computational fluid dynamic (CFD) models.

2.2 CFD modelling

CFD models solve the 3D mathematical flow equations to compute the fluid velocity vector and pressure at each cell of a computational mesh. Almost all CFD models (e.g. Fluent, Star-CCM+, CFX, OpenFOAM) use body-fitted meshes that conform to the external boundaries of solids present in computational domain. In this type of models, wave generation can be easily modelled if the slide is assumed as another fluid interacting with water (e.g Biscarini 2010). However, if the slide is modelled as a rigid non-deformable solid these models run into problems because the body-fitted mesh needs to be remeshed at every time step while the slide is moving, which can lead to numerical stabilities if mesh deformation is excessive. A possible way around is the use of overlapping or chimera meshes, which are small body-fitted meshes attached to the solid that move together inside a larger fixed body-fitted mesh. Another way is to avoid the use of body-fitted meshes altogether, as done by the CFD code Flow-3D.

2.3 Flow-3D

Flow-3D (www.Flow3D.com) uses a simple rectangular orthogonal mesh (Cartesian grid with rectangular prismatic cells). The solid is interpolated into the grid using the Fractional Area-Volume Obstacle Representation (FAVOR) method, in which a solid is allowed to cut through a cell and its location is recorded, not by moving the edges of the cell to conform to the solid as in body-fitted meshes, but in terms of the fractional face areas and fractional volume of the cell that are not covered by the solid. In this way, the grid and the solid remain independent of each other and it is easy to modify the solid while keeping the grid unchanged. This makes it easier for a moving solid, like a falling landslide, to move through a grid that remains invariant during the simulation (Das et al. 2009a; Basu et al. 2009a,b; Vasquez and de Lima 2016). Finally, another way to model landslide-generated waves without worrying about meshing issues is to use mesh-free numerical methods such as smoothed particle hydrodynamics (SPH).

2.4 SPH modelling

In SPH modelling, the fluid and solid are represented by discrete particles that interact with each other; but without the use of a computational mesh. SPH has been successfully applied to simulate wave generation and propagation (Das et al. 2009b; Heller et al. 2016). SPH is a very promising technique subject to very intense research, but at the moment it not as mature as CFD modelling for practical engineering applications.

3. FLOW-3D VALIDATION

3.1 Experimental data

Heller et al. (2016) conducted experiments of landslide-generated waves using the experimental setup shown in Figure 2. The experiment considered here was conducted in a two-dimensional arrangement, conducted within a straight flume 0.6 m wide, almost the same as the slide width such that waves propagate only along the 10 m long axis of the flume. The experiment with an initial water depth $h = 0.24$ m is considered here for Flow-3D validation (Figure 2).

Figure 2. Experimental setup of landslide-generated wave experiment (Heller et al. 2016, Spheric 2015).

Water levels in time were measured at 7 gauges located at distances between 3 and 35 times the water depth from the sloping bank (Figure 2). Figure 3 shows the wave height above the initial water surface, measured at the 7 gauges. The slide generates a solitary wave traveling away from the impact zone. The water surface elevation is most disturbed closer to the impact zone, with the water level not only rising above, but also being depressed below the initial surface. However, at a distance $35h$ (8.4 m) the wave exhibits almost perfect symmetrical solitary wave shape, with no disturbance below the water surface. Notably, there was little dissipation in the wave amplitude as it propagated away from the slide area.

Figure 3. Wave height in time measured at 7 gauges along the experimental flume ($h = 0.24$ m)

3.2 Flow-3D Setup

Modelling the slide movement in Flow-3D version 11.2 requires providing the spatial components of the both the linear and angular velocity of the moving slide. Heller et al. (2016) provide information on the "position" of the slide in time (Figure 2); whose exact meaning is not clear, as it could represent the distance along the curved surface of the slide slope or the distance along the cable-extension position transducer shown in Figure 2. For Flow-3D application, the experimental velocity magnitude (Figure 2) was decomposed by trial-and-error into the horizontal (V_x) and vertical (V_z) components, plus an angular velocity (ω_y) that approximated the velocity plot in Figure 2 assuming the slide followed the curved bottom trajectory. The geometry of the slide and circular bottom transition were provided by Spheric (2015). Initial water depth was assumed as $h = 0.24$ m with a hydrostatic pressure distribution. Friction was neglected. Turbulence was modelled using the RNG k-epsilon turbulence model. Preliminary 3D tests showed no improvement, so all runs were conducted in a 2D vertical plane. Total simulation time was 5.5 s. The domain was discretized using uniform grid cell sizes of 10 and 5 mm. Only the results with the fine 5 mm grid, which is considered mesh independent, are reported here. Flow-3D can solve the flow momentum equations using first order (FO), second order (SO) and second order monotonicity preserving (SOMP) numerical schemes; all of them were tested to assess their influence on the results, as discussed below.

3.3 Flow-3D results

Figure 3 shows the trajectory of the falling slide assumed in the simulation. The slide impacts the water surface at 2.4 m/s (Figure 3). The impact cause water to be displaced and gain kinetic energy, which leads to the generation and propagation of a single wave downstream.

3.3.1 First Order Momentum Advection

The results of Flow-3D using the default first order momentum advection numerical scheme are shown in Figure 6. The results are quite good near the slide area, up to a distance of 15h (3.6 m). However, beyond that distance the wave's shape deviates from the observed shape (Figure 5) becoming asymmetrical, longer and flatter.

3.3.2 Second Order Momentum Advection

In order to reduce numerical dissipation, another test was performed using the second order momentum advection as shown in Figure 8. Now the shape of the wave remains symmetrical as in the experiment, but the peaks near the slide are have decreased relative to the experiments (Figure 5) and previous results with the FO scheme (Figure 7).

The results obtained by Flow-3D when using the SOMP numerical scheme were not good and not presented here. However, it should be mentioned that when modelling flow over the flip bucket of Canyon Dam in the Peace River, Hurtig at al. (2013) found that the SOMP produced significant better results than the other momentum advection schemes. This finding highlights the importance of testing CFD model for various applications, as the prediction capabilities of their different numerical schemes may be problem-dependent.
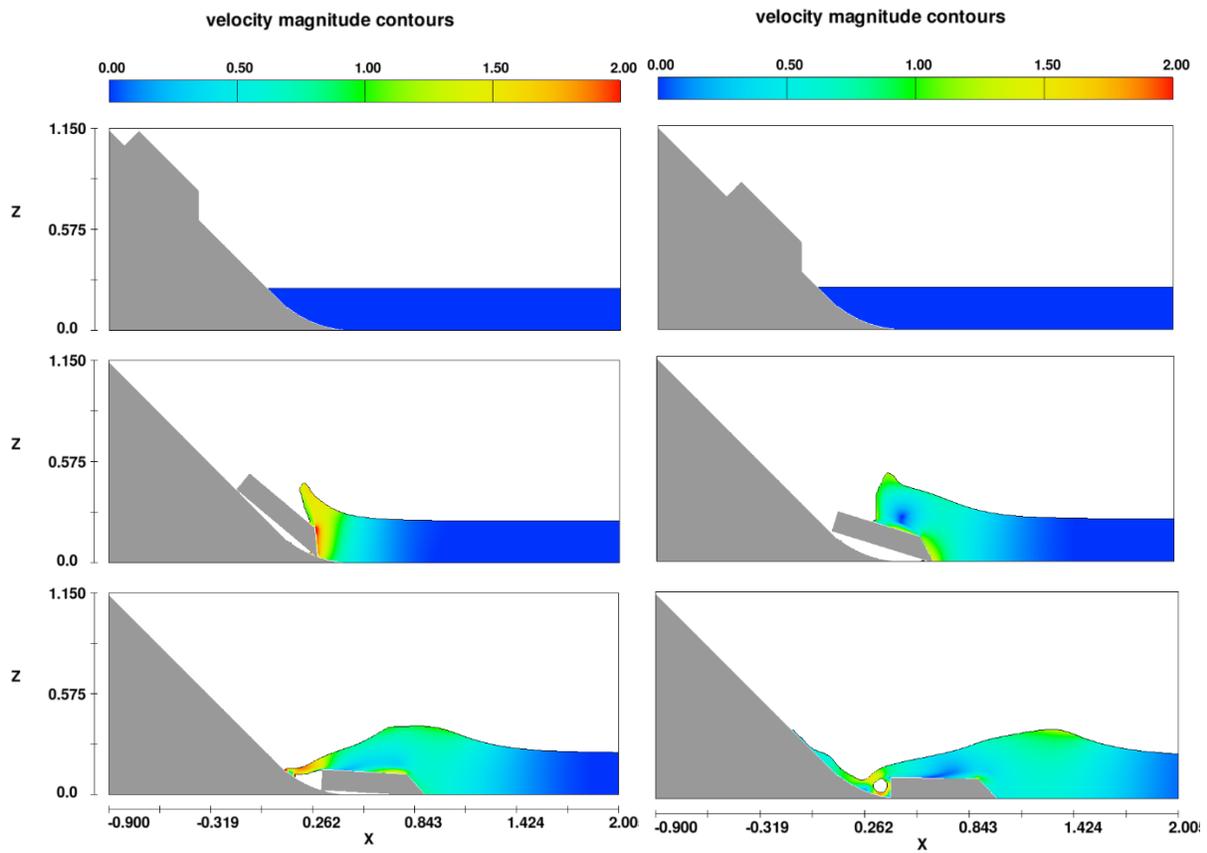
Figure 4. Time sequence showing trajectory of slide in Flow-3D
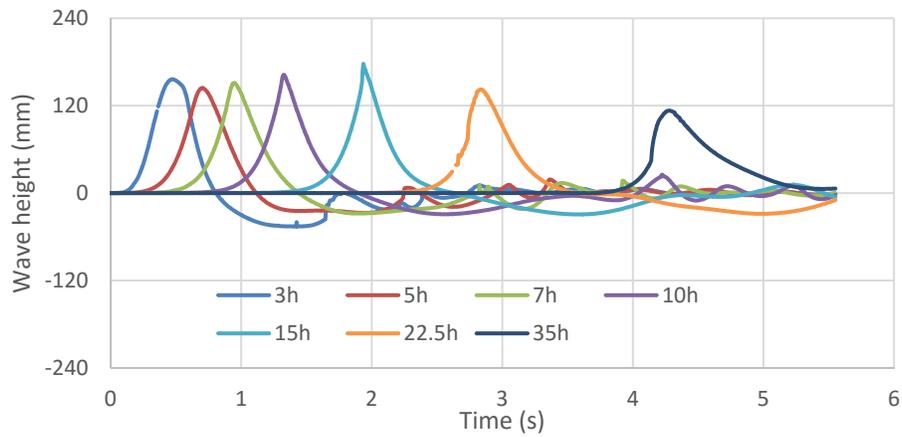
Figure 5. Flow-3D results using the default first order momentum advection numerical scheme
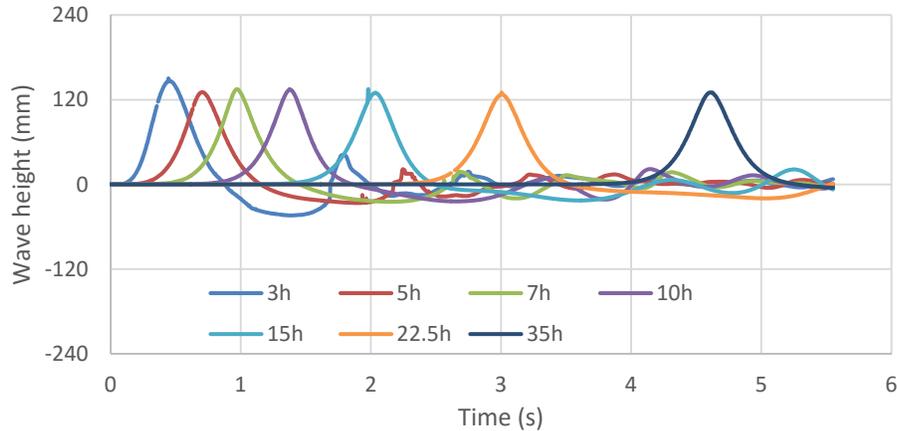
Figure 6. Flow-3D results using the second order momentum advection numerical scheme

4. WAVE PROPAGATION WITH IMPOSED BOUNDARY CONDITION

4.1 Hybrid approach?

Because conventional hydrodynamic models cannot simulate wave generation explicitly (phase 1 in Figure 1), they cannot be applied for landslide-generated wave modelling. However, when modelling the propagation of a sub-aqueous ocean tsunami using Telemac-2D, Horsburgh et al. (2008) did not simulate explicitly the tsunami wave generation, but instead assumed the initial tsunami wave and impose it as boundary condition in Telemac-2D to model wave propagation in the ocean. This raises the question of whether a similar approach could be applied for sub-aerial landslides. That is, a hybrid approach in which analytical wave generation equations are used to estimate the initial wave amplitude and length, and then that information is imposed as inflow boundary condition in a conventional hydrodynamic model to simulate the wave generation phase. The appeal of such an approach is that hydrodynamic models are more widely available and faster to run than CFD models.

In order to test this hypothesis, additional numerical models of Heller et al (2016) flume were developed using both River2D and Telemac-2D, but starting at $x = 3h = 0.72$ m and using a node spacing of 5 mm, similar to that of Flow-3D. The water levels measured in the experiment at $x = 3h$ were applied as inflow boundary condition. For comparison, as similar Flow-3D model was also developed and ran. Figure 7 shows the experimental results at $x = 35h$, compared with the numerical results of the various models. Telemac-2D offers several numerical schemes to choose from (see Figure 9); two of them which provided the highest wave amplitudes, the Harten-Lax-van Leer-Contact (HLLC) and Second Order Kinetic (SOK) schemes are shown in Figure 7.

All the numerical tests underpredicted the wave amplitude observed in the experiment (Figure 7). This is not completely unexpected, because the information on momentum transferred by the slide to water during the wave generation phase is not included in the simple time-varying water level used as inflow boundary condition. However, the high asymmetry of the predicted wave is harder to explain, considering that the imposed inflow wave at $x = 3h$ (Figure 3) is rather symmetrical. Although imposing a known water level inflow boundary condition to represent wave generation could be an acceptable approach for modelling sub-aqueous landslide-generated waves (Horsburgh et al. 2008); the numerical results shown in Figure 7 suggest this may not be true for the highly energetic sub-aerial landslide-generated waves, as the shape of the propagating wave gets significantly distorted for all numerical models tested.
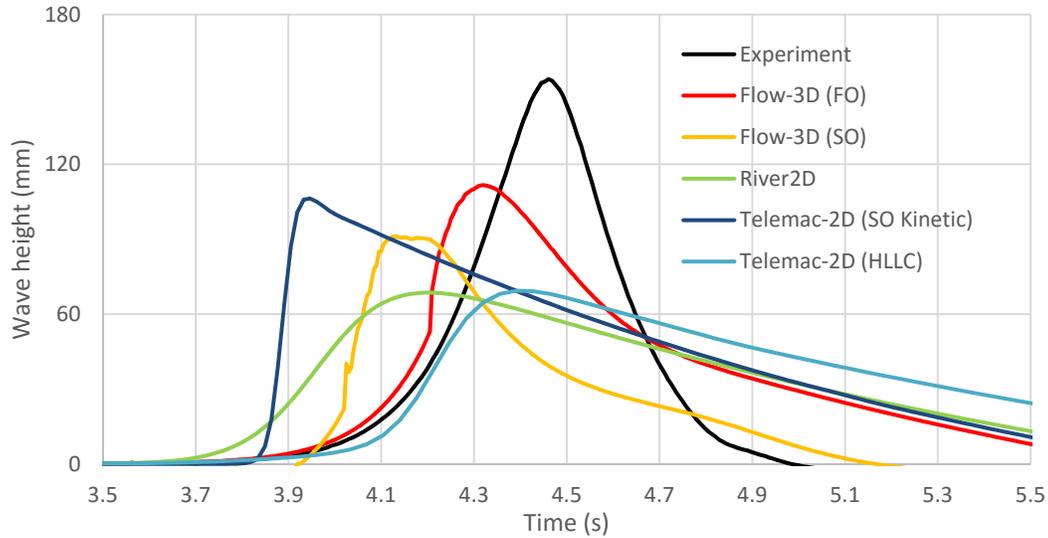
Figure 7. Wave height at $x = 35h$ predicted by various models assuming that wave at $x = 3h$ is known and imposed as inflow boundary conditions

4.2 Example in full scale reservoir

In order to illustrate the challenges of wave propagation modelling in a more realistic setting, a hypothetical example is presented here applying Telemac-2D in large $h = 42$ m deep reservoir. In this example, a single squared-sinusoidal wave with an amplitude of 18 m and period of 15 s is introduced at one shore of the reservoir. The wave propagates radially from its point of origin (slide location) with its amplitude decaying with distance as the wave propagates. The maximum wave amplitude predicted by Telemac-2D at an arbitrary point located 1.3 km away from the origin (a distance about $30h$) is reported in Figure 9 (for reference, when Flow-3D was applied for this case using a 5 m mesh and SO scheme, the maximum wave amplitude predicted was 5.5 m). Several simulations were performed in which the numerical scheme used to solve the equations or the mesh resolution were varied, while all other factors remained constant. The initial mesh with 30 m node spacing was refined first to 15 m and then again to 7.5 m.
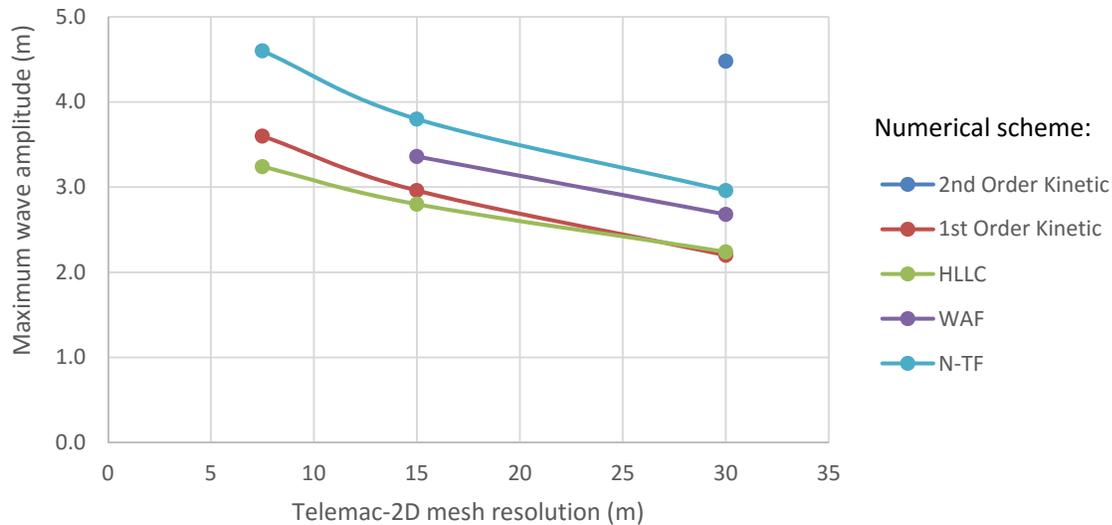
Figure 9. Influence of mesh resolution and numerical schemes used by Telemac-2D model on predicted wave maximum wave amplitude at point $30h$ away from hypothetical landslide location.

Figure 9 shows that predicted maximum wave amplitudes can be quite sensitive to the mesh resolution and adopted numerical scheme. Wave amplitude increased as the mesh was refined, regardless of the numerical scheme used, probably due to excessive numerical dissipation in the coarser meshes. The details of each numerical scheme used by Telemac-2D are not very relevant, but the important message here is that different approximations in the way the equations are solved lead to significantly different results when modelling wave propagation far from the point of wave generation. Since most numerical schemes tend to suffer from excessive dissipation (i.e. tend to underpredict wave amplitude), it could be argued that the SOK numerical scheme, which predicted the highest amplitudes for the 30 m mesh is perhaps less dissipative and hence more accurate (SOK also predicted the highest amplitude of Telemac-2D schemes tested in previous case, see Figure 7). But unfortunately, SOK became unstable in the finer 15 and 7.5 m meshes and results could not be obtained. The same was true for the WAF numerical scheme in the 7.5 m mesh. This illustrates another usual problem with numerical models, higher order or sophisticated schemes tend to be more problematic and cannot be applied in all practical cases.

5. SUMMARY AND CONCLUSIONS

Landslides falling into water bodies such as bays, fjords, rivers, lakes, mine pits and reservoirs have been observed to generate waves that can reach amplitudes tens of meters high (many of them in British Columbia); which can have devastating effects on human life and infrastructure. Therefore the need for reliable ways to predict wave amplitudes. In the case of numerical models, their predictions of maximum wave amplitudes are quite sensitive to the mesh resolution and numerical scheme chosen to solve the flow equations. For practical applications that require a high level of confidence in the predicted wave dynamics (e.g. significant risk to life and infrastructure), physical model is recommended. In lieu of physical modelling, CFD models with proven capabilities to explicitly simulate all the phases of landslide-generated waves (generation, propagation and runup), such as Flow-3D should be used.

This paper provides further evidence that Flow-3D can reproduce quite well the wave generation and propagation dynamics of sub-aerial landslide-generated waves caused by highly energetic slides falling in water. But in contrast with previous research that looked at wave generation and wave propagation in short flumes (Das et al. 2009a; Basu et al. 2009a,b; Vasquez and de Lima 2016), this paper extends those results to longer flumes where the choice of numerical scheme to solve the momentum equations can play a more important role in the prediction of wave propagation. In the case of Flow-3D, it was found that the First Order momentum advection scheme works well for wave generation and propagation near the landslide region. However, for distance beyond 10 times the water depth, the Second Order scheme is recommended for modelling wave propagation.

An alternative approach to model wave propagation using depth-averaged flow models is to assume the initial wave amplitude near the slide region as known and impose it as inflow boundary condition in the flow model. Although such an approach may work for sub-aqueous ocean tsunami waves (Horsburgh et al. 2008), it remains unproven for more energetic sub-aerial landslide-generated waves and its application is not recommended until fully validated. In general, the use of numerical models that have not been properly validated using experimental or field data specific to landslide-generated wave phenomena is not recommended.

6. REFERENCES

Ataie-Ashtani, B.; Nik-Khah, A. 2008. Impulsive waves caused by subaerial landslides. *Environmental Fluid Mechanics*, 8 (3): 263-280.

Biscarini, C. 2010. Computational fluid dynamics modelling of landslide generated water waves. *Landslides*, 7 (2): 117-124.

Basu, D., Green, S., Das, K., Janetzke, R.; Stamatakos, J. 2009a. Navier-Stokes simulations of surface waves generated by submarine landslides: effects of slide geometry and turbulence. 2009 *Society of Petroleum Engineers Americas Environmental & Safety Conference*, Santo Antonio, Texas.

Basu, D., Green, S., Das, K., Janetzke, R., and Stamatakos, J. 2009b. Numerical simulations of surface waves generated by subaerial landslide at Lituya Bay, Alaska. *28th International Conference on Ocean, Offshore and Artic Engineering*, Honolulu, Hawaii.

Clague, J.; Turner, B. 2006. *Vancouver, City on the Edge: Living with a Dynamic Geological Landscape.* Tricouni Press Ltd., Vancouver, BC.

Das, K., Green, S., Basu, D., Janetzke, R., and Stamatakos, J. 2009a. Effect of slide deformation and geometry on waves generated by submarine landslides: A numerical investigation. *2009 Offshore Technology Conference*, Houston, Texas, EEUU.

Das, K., Janetzke, R., Basu, D., Green, S., and Stamatakos, J. 2009b. Numerical simulations of Tsunami wave generation by submarine and aerial landslides using RANS and SPH. *28th International Conference on Ocean, Offshore and Artic Engineering*, Honolulu, Hawaii.

Flacker, G. and Eyzaguirre, V.R. 1979. Rock Avalanche and Wave at Chungar, Peru. *Rockslides and Avalanches, Vol. 2 Engineering Sites - Developments in Geotechnical Engineering*. Elservier Scientific Publishing Company, the Netherlands.

Fritz, H.M., Mohammed, F.; Yoo, J. 2009. Lituya Bay Landslide Impact Generated Mega-Tsunami 50th Anniversary. *Pure Applied Geophysics*, 166 (1-2): 153-175.

Heller, V., Hager, W. and Minor, H-E. 2009. *Landslide-generated waves in reservoirs- Basics and Computation.* ETH – Universidad de Zurich.

Heller, V., Bruggemann, M., Spinneken, J.; Rogers, B.D. 2016. Composite modelling of subaerial landslide-tsunami in different water body geometries and novel insight into slide and wave kinematics. *Coastal Engineering*, Vol. 109 (2016): 20-41.

Horsburgh, K. J., C. Wilson, B. J. Baptie, A. Cooper, D. Cresswell, R. M. W. Musson, L. Ottemöller, S., Richardson, and S. L. Sargeant 2008. Impact of a Lisbon-type tsunami on the U.K. coastline and the implications for tsunami propagation over broad continental shelves. *Journal of Geophysical Research: Oceans.* 13 (C4).

Hughes, B. R.; Berry, B.A. 1991. Landslide-generated waves. *Dam Safety* 1991.

Hurtig, K., Vasquez, J.A., and Croockweit. J. (2013). Verification of CFD Simulations of Flip Bucket Spillway Performance using Physical Model Results. *Canadian Dam Association 2013 Annual Conference*, Montreal, Canada, Oct. 5-10, 2013.

Miller, D.J. 1960. *Giant Waves in Lituya Bay, Alaska*. Geological Survey Professional Paper 354-C.

NHC 1976. *Hydraulic Model Study of Wave from Downie Slide*. Report prepared by Northwest Hydraulic Consultants Ltd. (NHC) for British Columbia Hydro and Power Authority, August 1976.

NHC 1983a. *Review of Landslide Generated Wave Analysis*, Report prepared by Northwest Hydraulic Consultants Ltd. (NHC) for British Columbia Hydro and Power Authority, May 1983.

NHC 1983b. *Peace River, Site C Project, Model of Landslide Waves at Attachie and Bear Flat Areas*. Report prepared by Northwest Hydraulic Consultants Ltd. (NHC) for BC Hydro, June 1983.

NHC 2005. *Checkerboard Creek Landslide Generated Wave – Physical Model Study*. Report prepared by Northwest Hydraulic Consultants Ltd. (NHC) for British Columbia Hydro and Power Authority, August 2005.

NHC 2012. *Análise Hidráulica de Movimentos de Massa nos Taludes da Mina de Águas Claras – CFD Simulation and Results*. Technical Memo prepared by Northwest Hydraulic Consultants Ltd. (NHC) for POTAMOS Engenharia e Hidrologia Ltda., July 2012.

NHC 2013. *Questa Mine Hydraulic Modelling of Landslide-Generated Waves*. Report prepared by Northwest Hydraulic Consultants Ltd. (NHC) for Golder Associates Inc., October 2013.

NHC 2016. *WSAP Mine Wave Hazard Assessment*. Report prepared by Northwest Hydraulic Consultants Ltd. (NHC) for Piteau Associates, April 2016.

Raney, D.C and Butler, H.L. 1975. *A Numerical Model for Prediction the Effects of Landslide-Generated Water Waves*. Hydraulics Laboratory, US Army Engineering Waterways Experiment Station. Report H-75-1.

SFU 2011. *Risky Ground*. Newsletter of Center for Natural Hazards, September 2011, Fall Edition. Simon Fraser University, Canada.

Slingerland, R. and Voight, B. 1982. Evaluating Hazard of Landslide-Induced Water Waves. *Journal of the Waterway, Port, Coastal and Ocean Division*, ASCE, Vol. 108, No. WW4, November 1982, pp. 504-512.

Spheric 2015. *Test 11: Subaerial landslide-tsunami generation with a rigid slide in a channel (2D) and basin (3D)*. https://wiki.manchester.ac.uk/spheric/index.php/Test11, last modified on 27 August 2015. Accessed on 5 February 2016.

Van Esch, K.J.B. 2012. *Failure Behaviour of Bedrock and Overburden Landslides of the Peace River Valley near Fort St. John, British Columbia.* Master's Thesis. University of British Columbia.

Vasquez, J.A.; de Lima, G. 2016. Modelación CFD de Ondas Tsunami en Reservorios, Lagos y Minas Causadas por Deslizamientos de Laderas. Proceedings of the *27th IAHR Latin American Conference*, Lima, Peru

Watson, A. D., Psutka, J. F., Stewart, T. W., and Moore, D. P. 2007. Investigations and monitoring of rock slopes at Checkerboard Creek and Little Chief Slide. In *1st Canada-US Rock Mechanics Symposium*. American Rock Mechanics Association, Vancouver, Canada.

Wikipedia 2016. Megatsunami. https://en.wikipedia.org/wiki/Megatsunami.